

# Variation of One-bond X–Y Coupling Constants ${}^1J(X-Y)$ and the Components of ${}^1J(X-Y)$ with Rotation about the X–Y Bond for Molecules $H_mX-YH_n$ , with X, Y = ${}^{15}N$ , ${}^{17}O$ , ${}^{31}P$ , ${}^{33}S$ : The Importance of Nonbonding Pairs of Electrons

Janet E. Del Bene<sup>\*,†</sup> and José Elguero<sup>‡</sup>

Department of Chemistry, Youngstown State University, Youngstown, Ohio 44555, and Instituto de Química Médica, CSIC, Juan de la Cierva, 3, E-28006 Madrid, Spain

Received: November 15, 2006; In Final Form: January 4, 2007

Ab initio EOM-CCSD calculations have been performed on molecules  $H_mX-YH_n$ , for X, Y =  ${}^{15}N$ ,  ${}^{17}O$ ,  ${}^{31}P$ , and  ${}^{33}S$ , to investigate the variation of one-bond X–Y spin–spin coupling constants  ${}^1J(X-Y)$  and the components of J with rotation about the X–Y single bond. The reduced Fermi-contact (FC) terms for all 10 molecules are negative and decrease in absolute value as the rotational angle  $\theta$  changes from  $0^\circ$ , at which point the lone pairs of electrons are on the same side of the X–Y bond, to  $180^\circ$  where they are trans with respect to the X–Y bond. The signs of reduced paramagnetic spin–orbit (PSO) and spin–dipole (SD) terms are opposite that of the FC term and exhibit extremum values as  $\theta$  approaches  $90^\circ$ , the gauche conformation. While the FC term tends to dominate for molecules  $H_2X-YH_2$  and  $H_2X-YH$ , such is not the case for  $HX-YH$ , where the PSO and SD terms assume increased importance. Curves for  ${}^1K(X-Y)$  as a function of rotational angle are readily grouped according to formula  $H_2X-YH_2$ ,  $H_2X-YH$ , and  $HX-YH$ , which suggests that it is the lone pairs of electrons on X and Y which are primarily responsible for the trends observed.

## Introduction

NMR spin–spin coupling constants are a powerful tool for investigating chemical bonds and molecular structure. If, in a molecule, X and Y are singly bonded and both are bonded to a reference atom A or B, then the geometry around the X–Y bond can be defined by the X–Y distance, the A–X–Y and X–Y–B angles, and the A–X–Y–B dihedral (torsion) angle  $\theta$ . It is intuitively clear that changes in the X–Y distance or in the A–X–Y and X–Y–B angles will change the one-bond X–Y coupling constant  ${}^1J(X-Y)$ . What is not obvious is how changes in the dihedral A–X–Y–B angle will affect  ${}^1J(X-Y)$  since the geometry of the X–Y bond itself is essentially unchanged as the dihedral angle changes. Nor is it obvious how variation in the dihedral angle will change two-bond couplings  ${}^2J(A-Y)$  and  ${}^2J(X-B)$ . However, if A and B are H atoms, then  ${}^3J(H-H)$  is known to depend on the dihedral angle  $\theta$ , a property which was discovered and given a theoretical justification by Karplus and which now deservedly bears his name.<sup>1,2</sup>

The question of how a one-bond coupling constant varies with dihedral angle led us to compute coupling constants for molecules  $H_2X-YH_2$ ,  $H_2X-YH$ , and  $HX-YH$ , for X, Y =  ${}^{15}N$ ,  ${}^{17}O$ ,  ${}^{31}P$ , and  ${}^{33}S$ . We observed Karplus-type variations in  ${}^1J(X-Y)$  as a function of dihedral angle and, in a recent letter,<sup>3</sup> reported the Karplus-type equations which were derived. In so doing, we demonstrated that even one-bond coupling constants in molecules with lone pairs of electrons on X and Y can vary significantly as the  $XH_m$  group is rotated about the X–Y bond. This is an important observation and represents an extension of the Karplus relationship for three-bond H–H coupling  ${}^3J(H-H)$  in H–C–C–H fragments. However, in ref 3, no data

were given to provide any insights into the interesting and varied behavior that was observed. Thus, it is the purpose of the present paper to expand and complete the study of the variation of  ${}^1J(X-Y)$  with dihedral angle by addressing the following questions: (1) How do the signs and magnitudes of the components of  ${}^1J(X-Y)$  vary with dihedral angle and which term or terms dominate? (2) Can trends in the variation of  ${}^1J(X-Y)$  and its components be identified? (3) Are the reduced coupling constants  ${}^1K(X-Y)$  for these molecules related, and if so, what determines this relationship?

## Methods

To determine the dependence of  ${}^1J(X-Y)$  on the dihedral angle, it is necessary to keep all of the geometrical parameters for each molecule fixed as this angle is varied for the calculation of coupling constants. To obtain a reasonable set of fixed geometrical parameters, the structures of these molecules were optimized at dihedral angles of  $0^\circ$  and  $180^\circ$ , and in some cases, the molecule was fully optimized, including the dihedral angle, if the equilibrium structure did not correspond to a value of  $0$  or  $180^\circ$  for that angle. Then, average values of all internal coordinates for these structures were obtained and were fixed for subsequent calculations of coupling constants as a function of the dihedral angle. The values of these coordinates are reported in Table 1. To examine the effect of freezing internal coordinates, the structure of HO–OH was also fully optimized at each dihedral angle, and  ${}^1J(O-O)$  values were computed for each structure. Geometry optimizations were carried out at second-order Møller–Plesset perturbation theory (MP2)<sup>4–7</sup> with the 6-31+G(d,p) basis set<sup>8–11</sup> for molecules in which X and Y are both second-period elements and with the aug-cc-PVTZ basis set<sup>12,13</sup> for molecules containing P and/or S. These optimizations were performed using the Gaussian03<sup>14</sup> suite of programs.

\* To whom correspondence should be addressed. E-mail: jedelbene@ysu.edu.

<sup>†</sup> Youngstown State University.

<sup>‡</sup> Instituto de Química Médica.

**TABLE 1: Distances (angstroms) and Angles (degrees) for Molecules  $H_mX-YH_n$** 

$H_mX-YH_n$	distances			angles			
	X-Y	X-H	Y-H	H-X-Y	X-Y-H	H-X-H	H-Y-H
$H_2N-NH_2$	1.460	1.015	1.015	107.5	107.5	106.0	106.0
$H_2N-PH_2$	1.763	1.013	1.417	110.6	98.0	106.1	91.8
$H_2P-PH_2$	2.252	1.414	1.414	95.0	95.0	92.6	92.6
$H_2N-OH$	1.452	1.017	0.966	101.9	103.4	106.2	
$H_2N-SH$	1.718	1.011	1.346	111.1	99.5	108.8	
$H_2P-OH$	1.670	1.417	0.963	99.6	110.0	92.4	
$H_2P-SH$	2.219	1.412	1.338	98.2	96.4	93.8	
HO-OH	1.477	0.970	0.970	100.0	100.0		
HO-SH	1.692	0.965	1.339	106.6	96.8		
HS-SH	2.099	1.338	1.338	95.5	95.5		

**TABLE 2: One-bond Coupling Constants (J) and Components of J (Hz) for Molecules  $CH_3-CH_3$ ,  $CH_3OH$ , and  $CH_3SH$** 

		$H_3C-CH_3^a$			$^1J(C-C)$
$\theta$	PSO	FC	SD		
0	0.7	35.1	1.1	37.0	
20	0.5	35.1	1.1	36.9	
40	0.3	35.2	1.0	36.6	
60	0.2	35.2	1.0	36.5	
		$CH_3OH^b$			$^1J(C-O)$
$\theta$	PSO	FC	SD		
0	-3.1	19.2	-2.2	13.9	
20	-3.0	19.3	-2.2	14.0	
40	-2.9	19.3	-2.1	14.2	
60	-2.8	19.3	-2.1	14.3	
		$CH_3SH^b$			$^1J(C-S)$
$\theta$	PSO	FC	SD		
0	2.7	-10.6	2.2	-5.7	
20	2.6	-10.7	2.2	-5.9	
40	2.4	-10.7	2.1	-6.2	
60	2.3	-10.7	2.1	-6.3	

<sup>a</sup> C-H bonds eclipsed at  $\theta = 0^\circ$  and staggered at  $\theta = 60^\circ$ . <sup>b</sup> The O-H and S-H bonds eclipse a C-H bond at  $\theta = 0^\circ$  and are staggered with respect to the C-H bonds at  $\theta = 60^\circ$ .

Ab initio spin-spin coupling constants were computed using the equation-of-motion coupled-cluster singles and doubles method (EOM-CCSD) in the CI (configuration interaction)-like approximation<sup>15-18</sup> with all electrons correlated, using the Ahlrichs qzp basis set on N and O and the qz2p basis on H, P, and S.<sup>19</sup> This level of theory gives computed coupling constants in agreement with experiment, without any rescaling of the computed values. For these calculations, the dihedral angle ( $\theta$ ) was set to  $0^\circ$  and then incremented to  $180^\circ$  in steps of  $20^\circ$ . At each value of  $\theta$ , the total coupling constant  $^1J(X-Y)$  was evaluated as a sum of four terms:<sup>20</sup> the paramagnetic spin-orbit (PSO), diamagnetic spin-orbit (DSO), Fermi-contact (FC), and spin-dipole (SD), using the ACES II program.<sup>21</sup> All calculations were carried out at the Ohio Supercomputer Center on the Cray X1 or the Itanium cluster.

The terms that may make significant contributions to  $^1J(X-Y)$  for the 10 molecules investigated in this study are the PSO, FC, and SD terms. From a sum-over-states perspective,<sup>20</sup> the FC term arises from coupling between the ground state and excited triplet states, since the operator for the FC term contains spin. The FC term is a contact term and thus depends on  $\sigma$ -electron densities at the coupled nuclei. The PSO and SD operators do not contain spin, and therefore, it is excited singlet states which couple to the ground state. Both terms depend upon the distribution of electrons other than  $\sigma$ . The PSO term arises

from orbital currents induced by the magnetic fields of the nuclei, while the SD term results from the spin polarization caused by the magnetic dipole field of the nuclear moment. As will become obvious below, these terms can vary significantly as the dihedral angle changes.

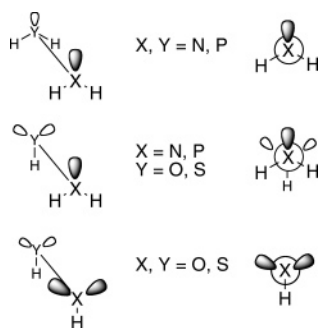
## Results and Discussion

Before discussing the variation of  $^1J(X-Y)$  and its components for the 10 molecules investigated in this study, it is advantageous to consider how these terms vary as a function of dihedral angle for  $H_3C-CH_3$  with no lone pairs of electrons and  $H_3C-OH$  and  $H_3C-SH$  which have two lone pairs on O and S, respectively, but none on C. The data required for this analysis are reported in Table 2. From these data, it can be seen that  $^1J(C-C)$  for  $H_3C-CH_3$  is dominated by the FC term, which is essentially constant as the dihedral angle changes. Both the PSO and SD terms are small, with the SD remaining essentially constant and the PSO term decreasing by 0.5 Hz as one  $CH_3$  group rotates from an eclipsed conformation at  $\theta = 0^\circ$ , to a staggered conformation at  $\theta = 60^\circ$ . The computed values of  $^1J(C-C)$  are in agreement with the experimental value of 34.6 Hz.<sup>22</sup>

Introducing lone pairs on one atom leads to notable changes in the total coupling constants  $^1J(C-O)$  and  $^1J(C-S)$  and their components. For both  $H_3C-OH$  and  $H_3C-SH$ , the FC terms still dominate and remain essentially constant as the dihedral angle changes. However, the PSO and SD terms assume increased importance and are of opposite sign relative to the FC term. The PSO term decreases slightly in absolute value as  $\theta$  increases, while the SD term remains relatively constant. For both  $H_3C-OH$  and  $H_3C-SH$ , there is a small decrease in the total coupling constant as the O-H and S-H bonds rotate from an eclipsed to a staggered conformation relative to the C-H bonds, although this variation is less than 1 Hz. Finally, the reduced FC terms and reduced total coupling constants for these two molecules are negative. Thus, the presence of lone pairs of electrons on O or S is sufficient to change the sign of the reduced FC terms and the reduced coupling constants from positive in  $H_3C-CH_3$  to negative in  $H_3C-OH$  and  $H_3C-SH$  and to make the signs of the PSO and SD terms opposite that of the FC term.

Having described total J and its components as a function of dihedral angle for molecules  $H_3C-CH_3$ ,  $H_3C-OH$ , and  $H_3C-SH$ , it is now appropriate to return to the behavior of the one-bond X-Y coupling constants for the 10 molecules investigated in this study. To facilitate analysis of coupling constants as a function of dihedral angle for molecules with lone pairs of electrons on X and Y, the conformations corresponding to a dihedral angle of  $0^\circ$  were defined as shown in Chart 1. For molecules  $H_2X-YH_2$ , at  $\theta = 0^\circ$ , the bisectors of the H-X-H and H-Y-H angles define a plane and are "cis" to each other

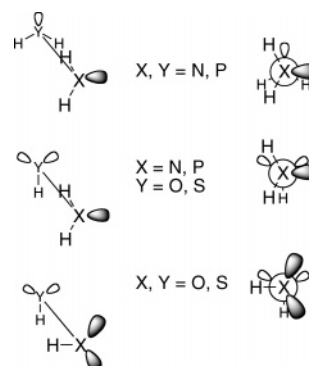
CHART 1



with respect to the X–Y line. Relative to the bisectors, the lone pairs of electrons on X and Y lie on the opposite side of the X–Y bond, cis to each other and in an “eclipsed” conformation, as indicated in Chart 1. For molecules  $H_2X-YH$ , a dihedral angle of  $0^\circ$  places the bisector of the H–X–H angle and the Y–H bond “cis” to each other. The lone pairs on X and Y are then oriented as shown in Chart 1. In this orientation, the two lone pairs on Y are equivalent and together in closest proximity to the lone pair on X. Finally, the “cis” orientation of X–H and Y–H bonds defines a dihedral angle of  $0^\circ$  for molecules  $HX-YH$ , as illustrated in Chart 1. The lone pairs on X and Y are eclipsed and in closest proximity at  $\theta = 0^\circ$ . The PSO, FC, and SD terms and  $^1J(X-Y)$  values as a function of the dihedral angle for the 10 molecules investigated in this study are reported in Table S1 of the Supporting Information.

**Variation of Coupling Constants for Molecules  $H_2X-YH_2$ .**  $H_2N-NH_2$ . Figure 1 illustrates the variation of the FC term and  $^1J(N-N)$  as a function of the dihedral angle  $\theta$  for  $H_2N-NH_2$ . It is evident that the shape of the  $^1J(N-N)$  curve is that of the FC curve. The FC term itself is always negative and has its greatest absolute value when  $\theta$  is  $0^\circ$  and the lone pairs are in closest proximity, “cis” with respect to the X–Y bond. Thus, both the FC term and  $^1J(N-N)$  decrease in absolute value as  $\theta$  increases from 0 to  $180^\circ$ . Since this behavior was not seen for  $H_3C-CH_3$ ,  $H_3C-OH$ , and  $H_3C-SH$ , the decrease in the FC term as the dihedral angle increases may be attributed primarily to the presence of the lone pairs on the two N atoms and their relative orientation. Once again, the PSO and SD terms are relatively small and positive. However, while they exhibit only a relatively small variation with dihedral angle, both terms decrease and have a minimum value near  $\theta = 90^\circ$ . In the context of molecular geometries, an equilibrium geometry at this conformation is referred to as the gauche geometry, a result of the “gauche effect, a tendency for a molecule to adopt that structure which has the maximum number of gauche interactions between the adjacent electron pairs and/or polar bonds”.<sup>23</sup> The gauche effect has been associated with a dihedral angle of about  $90^\circ$  for the equilibrium conformation of  $H_2N-NH_2$ .<sup>24</sup> (The computed MP2/6-31+G(d,p) value of this angle for the equilibrium structure is  $91^\circ$ .) In this paper, conformations in the region surrounding  $\theta = 90^\circ$  will be referred to as gauche conformations and are illustrated in Chart 2. It has been noted previously that the gauche effect is related to the anomeric effect.<sup>2,25</sup>

It is apparent that the PSO and SD terms make relatively small contributions to the total coupling constant at small values of the dihedral angle, but at large angles as the FC term decreases, the positive PSO and SD terms make  $^1J(N-N)$  small but positive. It is interesting to note that  $^1J(N-N)$  is negative for most values of  $\theta$ , which means that the reduced coupling constant  $^1K(N-N)$  is also negative, and therefore an exception

CHART 2: Gauche Conformation at  $\theta = 90^\circ$ 

to the Dirac Vector Model,<sup>26</sup> which states that reduced one-bond coupling constants are positive. From a sum-over-states perspective, the sign of the FC term is determined by a competition between triplet excited states which couple to the ground state and make positive contributions to the FC term (the nuclear magnetic moments are antiparallel) and those which make negative contributions (parallel nuclear magnetic moments). The NMR Triplet Wavefunction Model (NMRTWM)<sup>27</sup> suggests that nodal properties of the dominant excited states change as the orientation of the lone pairs changes. This is a recurring theme for all molecules  $H_mX-YH_n$ .

$H_2N-PH_2$ . The curves showing the variation of the FC term and  $^1J(P-N)$  for  $H_2N-PH_2$  have shapes similar to those shown for  $H_2N-NH_2$  in Figure 1. However, since the magnetogyric ratios of  $^{15}N$  and  $^{31}P$  have opposite signs, both the FC term and total  $^1J(P-N)$  are positive for all values of the dihedral angle. (The similarity of these curves will be evident when the curves for the reduced coupling constants for  $H_2N-NH_2$  and  $H_2N-PH_2$  are compared.) FC and  $^1J(P-N)$  are largest at  $\theta = 0^\circ$  and decrease as  $\theta$  increases. As evident from Table S1, the PSO and SD terms are relatively small and negative at all angles and exhibit their minimum absolute values at the gauche conformation.

$H_2P-PH_2$ . Figure 2 depicts the variation of  $^1J(P-P)$  and the terms that contribute to this coupling constant as a function of dihedral angle  $\theta$ . In contrast to  $H_2N-NH_2$  and  $H_2N-PH_2$ , the PSO and SD terms each make relatively large contributions of about 50 Hz to  $^1J(P-P)$  at  $\theta = 0^\circ$ . However, the PSO term decreases rapidly with increasing  $\theta$ , has its minimum value of 14 Hz at the gauche conformation, and then varies between 14 and 18 Hz as  $\theta$  increases to  $180^\circ$ . The contribution of the SD term varies between 46 and 53 Hz over the entire range of dihedral angles but also has its minimum absolute value near the gauche conformation. Since the signs of the PSO and SD terms are again opposite that of the FC term and the rates at which these terms change as a function of  $\theta$  are different,  $^1J(P-P)$  exhibits a maximum absolute value at a dihedral angle of  $60^\circ$ , and then decreases, changes sign, and becomes slightly positive (5 Hz) when the PSO and SD terms dominate at  $\theta = 180^\circ$ . The increased importance of the PSO term especially when the lone pairs are eclipsed, and of the SD term over the entire range of dihedral angles, may arise from the presence of high-lying occupied orbitals associated with the phosphorus lone pairs and low-lying virtual orbitals, which combine to form excited singlet states that interact strongly with the ground state.

**Variation of Coupling Constants for Molecules  $H_2X-YH$ .** Coupling constants  $^1J(X-Y)$  for molecules  $H_2N-OH$ ,  $H_2N-SH$ ,  $H_2P-OH$ , and  $H_2P-SH$  which have two lone pairs on Y and one on X are dominated by the FC term. The variation of the PSO, FC, and SD terms and  $^1J(N-O)$  for  $H_2N-OH$  as a

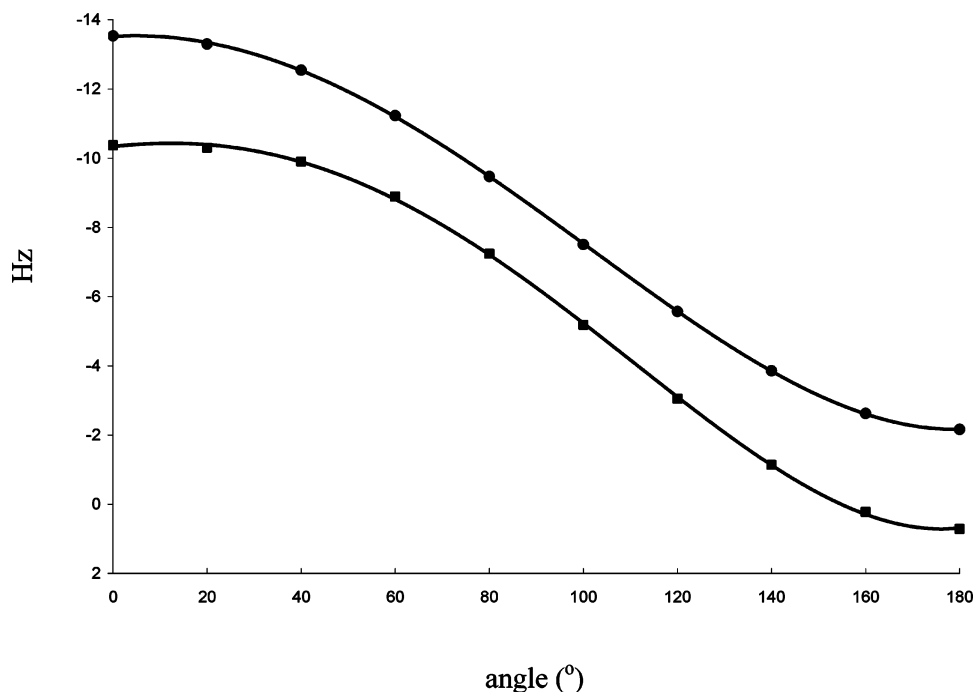


**Figure 1.** Variation of  ${}^1J(X-Y)$  (■) and the FC (●) term with torsion angle for  $H_2N-NH_2$ .

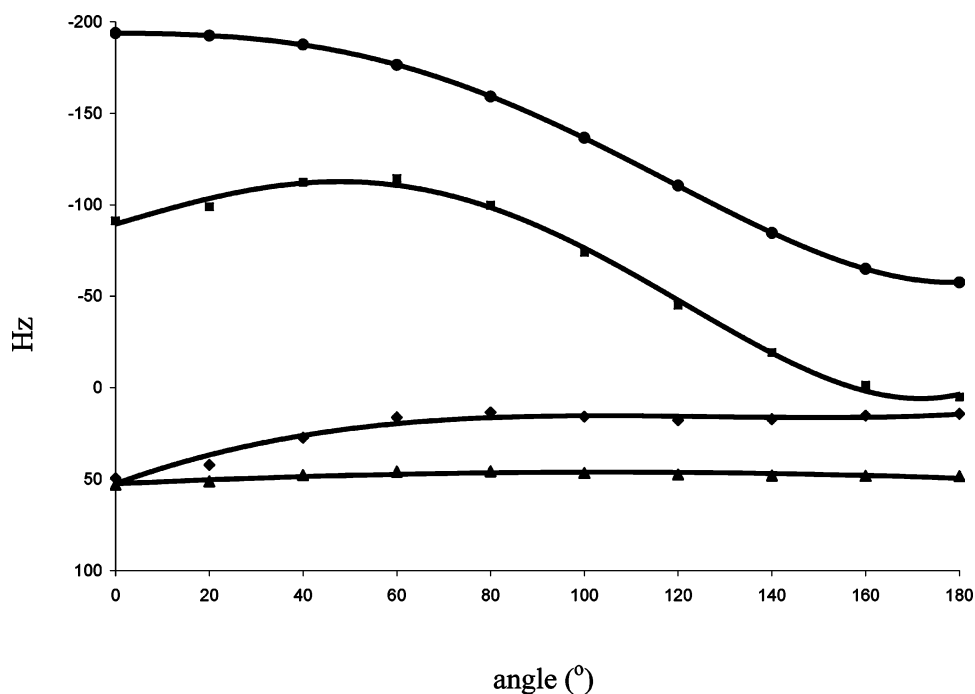


**Figure 2.** Variation of  ${}^1J(X-Y)$  (■) and FC (●), PSO (◆), and SD (▲) terms with torsion angle for  $H_2P-PH_2$ .

function of  $\theta$  can be seen in Figure 3, which illustrates that the shape of the  ${}^1J(N-O)$  curve is essentially the shape of the FC curve. The corresponding curves for  $H_2N-SH$  and  $H_2P-OH$  are similar, although the signs of the FC terms and  ${}^1J(X-Y)$  are positive because of the differences in the signs of the magnetogyric ratios of the coupled atoms. In contrast to molecules  $H_2X-YH_2$ , the PSO and SD terms have their greatest absolute values at the gauche conformation. Nevertheless, the FC term dominates at all angles, and the sign of  ${}^1J(X-Y)$  is the sign of the FC term.

The corresponding plots for  $H_2P-SH$  are given in Figure 4. For this molecule, the FC term is negative and decreases in absolute value with increasing  $\theta$ . The PSO and SD contributions are positive and have increased significance, particularly in the

region surrounding the gauche conformation where they have their maximum values. Nevertheless, the sign of  ${}^1J(P-S)$  is the same as the sign of the FC term for all values of  $\theta$ . For all molecules in this set, the signs of the PSO and SD terms are opposite that of the FC term, and the reduced FC terms and reduced  $X-Y$  coupling constants are always negative.

**Variation of Coupling Constants for Molecules  $HX-YH$ .** There are interesting differences in total coupling constants and terms which contribute to these for molecules  $HX-YH$  compared with  $H_2X-YH_2$  and  $H_2X-YH$ .

**HO-OH.** Figure 5 shows PSO, SD, and FC terms and  ${}^1J(O-O)$  for  $HO-OH$  as a function of the  $H-O-O-H$  dihedral angle. Once again, the signs of the PSO and SD terms are opposite that of the FC term. However, the PSO term is positive

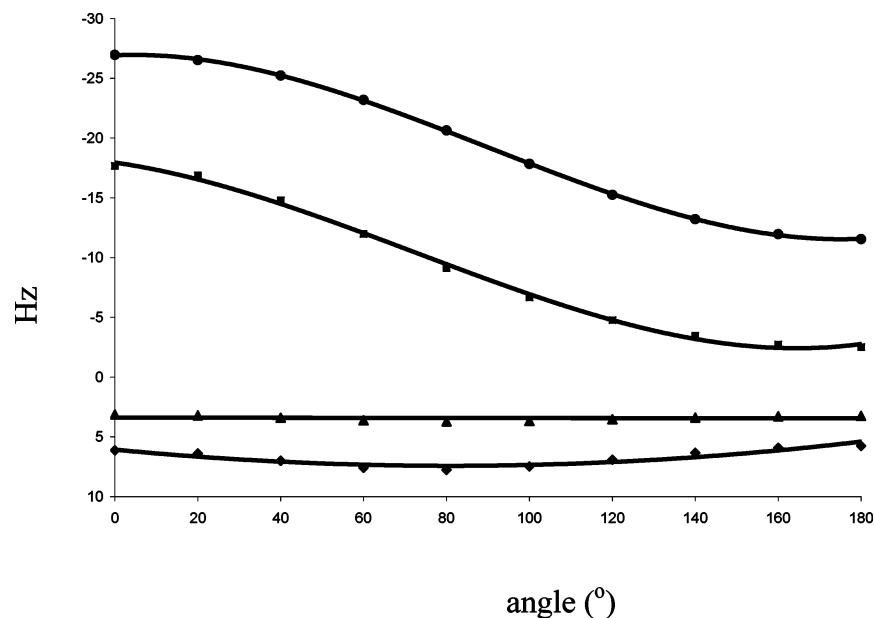


Figure 3. Variation of  $^1J(X-Y)$  (■) and FC (●), PSO (◆), and SD (▲) terms with torsion angle for  $H_2N-OH$ .

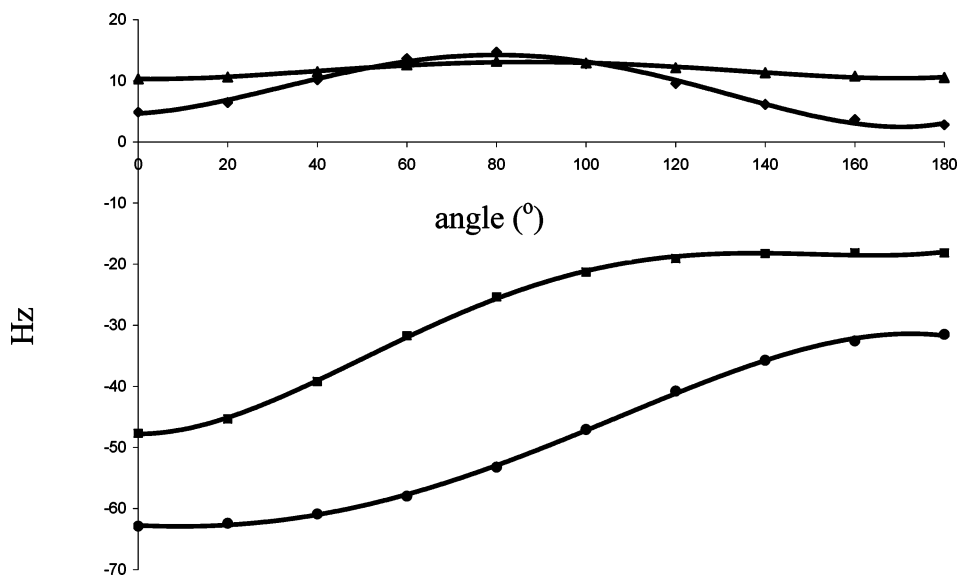


Figure 4. Variation of  $^1J(X-Y)$  (■) and FC (●), PSO (◆), and SD (▲) terms with torsion angle for  $H_2P-SH$ .

and greater than the absolute value of the FC term at all values of the dihedral angle. This term along with the SD term dominate the FC term, which decreases in absolute value as  $\theta$  increases, with the result that  $^1J(O-O)$  is positive over the entire range of dihedral angles. Both the PSO and SD terms exhibit minimum values at the gauche conformation and have similar values at 0 and 180°. These variations are reflected in the  $^1J(O-O)$  curve, which has its minimum value in the gauche region, and its largest value when  $\theta$  is 180° and the lone pairs are trans with respect to the O–O bond. At this value of the dihedral angle, the PSO and SD terms are large and positive, while the FC term has decreased to its smallest negative value.

In a recent paper, Gräfenstein and Cremer<sup>28</sup> noted that while the FC term probes the  $\sigma$ -electron structure of a molecule, the PSO and SD terms probe the  $\pi$ -electron structure. Application of their description to HO–OH provides some insight into the variation of these noncontact terms with dihedral angle. Consider the  $z$ -axis of HO–OH as co-incident with the O–O bond and let the  $x$ - $z$  plane be the plane of the molecule when  $\theta = 0$  and 180°. At these two conformations, HO–OH has a well-defined  $\pi$  system ( $\pi_y$ ) and also a pseudo- $\pi$  system in the plane of the

molecule (pseudo- $\pi_x$ ). As  $\theta$  increases from 0 to 180°, these  $\pi$  systems are at first perturbed and then essentially destroyed at the gauche conformation. Since the PSO and SD terms are largest when  $\theta$  is 0 and 180°, and smallest at the 90° gauche conformation, these results support the statement made in ref 28, namely, that the PSO and SD terms may be useful for describing the  $\pi$  character of covalent bonds. However, since the PSO and SD terms are at a maximum at the gauche conformation for molecules  $H_2X-YH$  but at a minimum for molecules  $HX-YH$ , further investigations into the relationship between these terms and the presence of  $\pi$  and/or pseudo- $\pi$  bonds and their variation with dihedral angle are warranted. In this context, it should also be noted that in a study of  $H_3C-OH$ , Pecul and Helgaker observed that the three-bond coupling constant  $^3J(H-H)$  becomes negative as the dihedral angle approaches 90°. <sup>29</sup>

Figure 6 shows plots of  $^1J(O-O)$  and the FC terms for HO–OH at the fixed geometry used for this study and at geometries which were optimized at each dihedral angle. The shapes of the two  $^1J(O-O)$  curves are similar, although at  $\theta = 0^\circ$ ,  $^1J(O-O)$  for the frozen geometry is greater than  $^1J(O-O)$  for

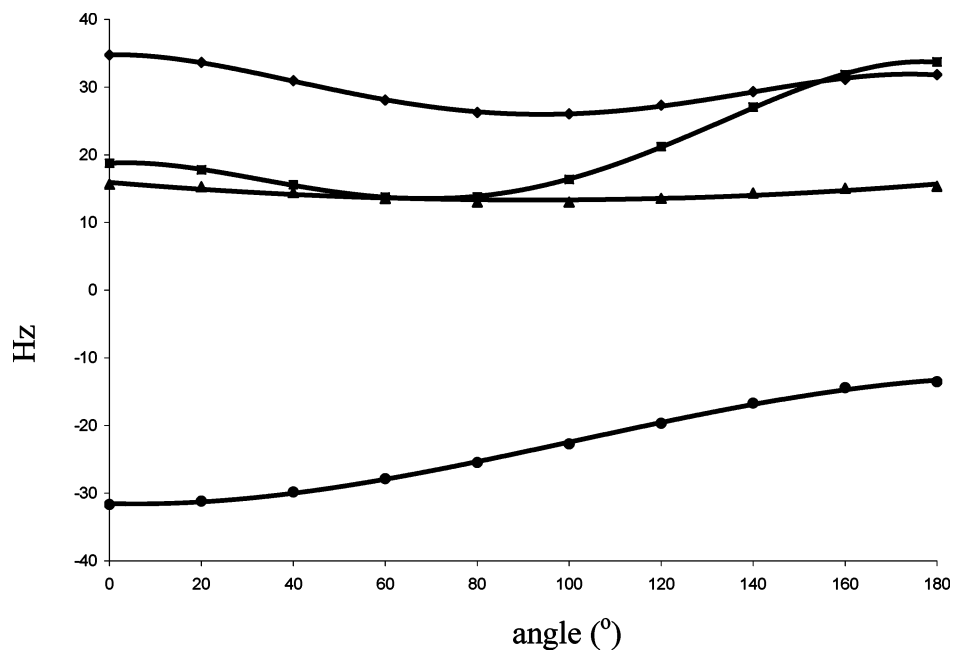


**Figure 5.** Variation of  ${}^1J(X-Y)$  (■) and FC (●), PSO (◆), and SD (▲) terms with torsion angle for HO–OH.

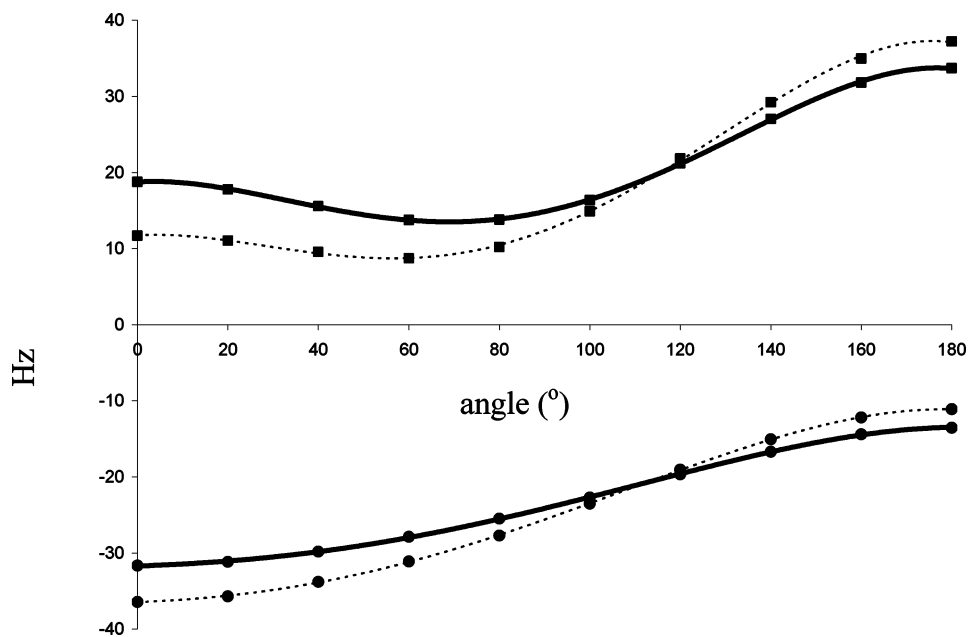


**Figure 6.** Variation of  ${}^1J(X-Y)$  (■) and FC (●) terms with torsion angle for HO–OH at the frozen geometry (solid lines) and at the optimized geometry at each dihedral angle (dashed lines).

the fixed, whereas at  $\theta = 180^\circ$  the opposite is true. These differences are directly attributable to differences in the FC terms, since FC for the frozen geometry is less negative at  $\theta = 0^\circ$  but more negative when  $\theta = 180^\circ$ . The PSO and SD curves are very similar at frozen and optimized geometries. This comparison suggests that freezing the internal coordinates while evaluating  ${}^1J(X-Y)$  as a function of dihedral angle does not introduce any anomalies into the results of these calculations.

**HO–SH.** Figure 7 shows PSO, SD, and FC terms and  ${}^1J(S-O)$  for HO–SH as a function of  $\theta$ . The pattern of changes in PSO, SD, and FC terms observed for HO–OH is evident once again. However, the PSO and SD terms are not as large relative to the FC term for the mixed second–third period molecule HO–SH compared with HO–OH, and there is a near cancellation of PSO and SD terms with the FC term. As a result,  ${}^1J(S-O)$  has an absolute value of less than 10 Hz over the entire range of dihedral angles. Its maximum value of +7.4 Hz is

found for the gauche conformation at which point the PSO and SD terms have their minimum negative values and the FC term dominates. As  $\theta$  increases, the FC term decreases and the PSO and SD terms increase, making  ${}^1J(S-O)$  negative at  $\theta = 180^\circ$ . The competition between the terms which contribute to  ${}^1J(S-O)$ , and the maximum in this curve near  $\theta = 90^\circ$ , are evident from Figure 7.

**HS–SH.** Figure 8 and Table S1 report variations in PSO, FC, and SD terms and  ${}^1J(S-S)$  as a function of dihedral angle. Once again, both the PSO and SD terms are positive, have their smallest values at the gauche conformation, and are largest when  $\theta$  is 0 and  $180^\circ$ . The FC term is of opposite sign and decreases as  $\theta$  increases. The net result is that  ${}^1J(S-S)$  is essentially 0 Hz at  $90^\circ$  and has its largest positive values when the PSO and SD terms dominate at  $0^\circ$  (9 Hz) and  $180^\circ$  (11 Hz), at which angles the  $\pi$  system is well-defined. However, the competition between the PSO and SD terms with the FC term results in a

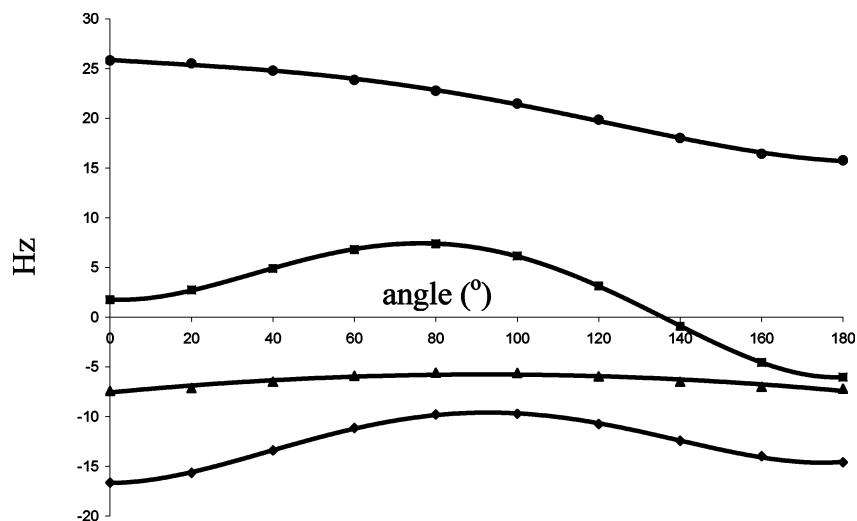


Figure 7. Variation of  ${}^1J(X-Y)$  (■) and FC (●), PSO (◆), and SD (▲) terms with torsion angle for HO–SH.

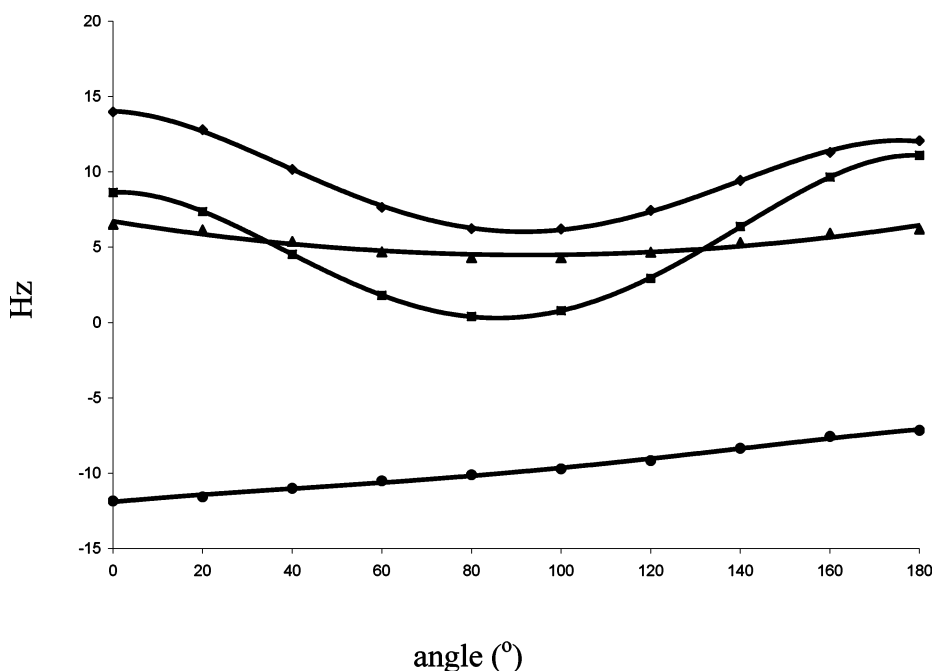


Figure 8. Variation of  ${}^1J(X-Y)$  (■) and FC (●), PSO (◆), and SD (▲) terms with torsion angle for HS–SH.

relatively small S–S coupling constant over the entire range of dihedral angles. The shape of the  ${}^1J(S-S)$  curve is very similar to the shape of the PSO curve, as evident from Figure 8.

At this point, it would be appropriate to compare the computed coupling constants with experimental data. Unfortunately, there is a scarcity of such data, and coupling constants have not been measured for any of the 10 molecules investigated in this work. The most closely related molecules are derivatives, such as  $(C_6H_5)HN-NH_2$ , for which the experimentally measured  ${}^{15}N-{}^{15}N$  coupling constant is  $-6.7$  Hz.<sup>30</sup> This value corresponds to a value of  $84^\circ$  for the dihedral angle computed from the Karplus equation for  $H_2N-NH_2$ .  ${}^1J(P-N)$  has been measured for  $(CH_3)_2N-P(CH_3)_2$  (60 Hz) and  $(C_6H_5)HN-PH(C_6H_5)$  (53 Hz).<sup>31</sup> These experimental values correspond to computed values of  ${}^1J(P-N)$  for  $H_2N-PH_2$  at small dihedral angles. Finally,  ${}^1J(P-P)$  has been determined experimentally for  $(CH_3)_2P-P(CH_3)_2$  ( $-180$  Hz) and  $(C_6H_5)HP-PH(C_6H_5)$  ( $-191$  Hz).<sup>32</sup> The largest computed values of  ${}^1J(P-P)$  for  $H_2P-PH_2$  are only  $-114$  Hz. Either the calculations significantly underestimate the P–P coupling constant or the substituents significantly increase  ${}^1J(P-P)$ .

${}^1K(X-Y)$  for  $H_mX-YH_n$ . To compare coupling constants involving different atoms, it is necessary to use the reduced coupling constants  ${}^1K(X-Y)$ ,

$${}^1K(X-Y) \propto {}^1J(X-Y)/(\gamma_X)(\gamma_Y)$$

where  $\gamma_X$  and  $\gamma_Y$  are the magnetogyric ratios of atoms X and Y ( ${}^{15}N$  and  ${}^{17}O$  negative;  ${}^{31}P$  and  ${}^{33}S$  positive). A comparison of the variation of  ${}^1K(X-Y)$  with dihedral angle is most informative if done according to formula  $(H_2X-YH_2, H_2X-YH, HX-YH)$ . Figure 9 shows the variation of  ${}^1K(N-N)$ ,  ${}^1K(N-P)$ , and  ${}^1K(P-P)$  for  $H_2N-NH_2$ ,  $H_2N-PH_2$ , and  $H_2P-PH_2$ , respectively, as a function of dihedral angle. The shapes of the  ${}^1K(N-N)$  and  ${}^1K(N-P)$  curves are similar over the entire range of  $\theta$  values, but the curve for  ${}^1K(P-P)$  is different for  $\theta$  less than  $90^\circ$ . The extremum found in the  ${}^1K(P-P)$  curve at  $60^\circ$  may be attributed to the decreased positive contributions of PSO and SD terms to P–P coupling in the region surrounding the gauche conformation. At an angle of  $0^\circ$  when the lone pairs on X and Y are in a cis “eclipsed” conformation,  ${}^1K(X-Y)$  for the mixed second–third period molecule  $H_2N-PH_2$  has the

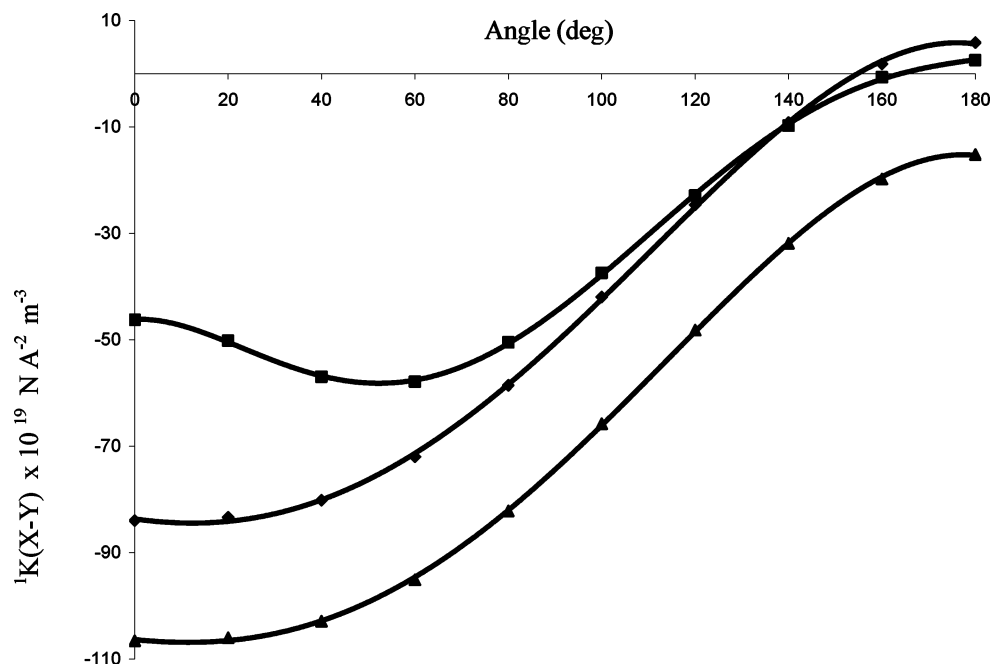


**Figure 9.** Variation of  ${}^1K(X-Y)$  for  $\text{H}_2\text{N-NH}_2$  (◆),  $\text{H}_2\text{N-PH}_2$  (▲), and  $\text{H}_2\text{P-PH}_2$  (■) with torsion angle.

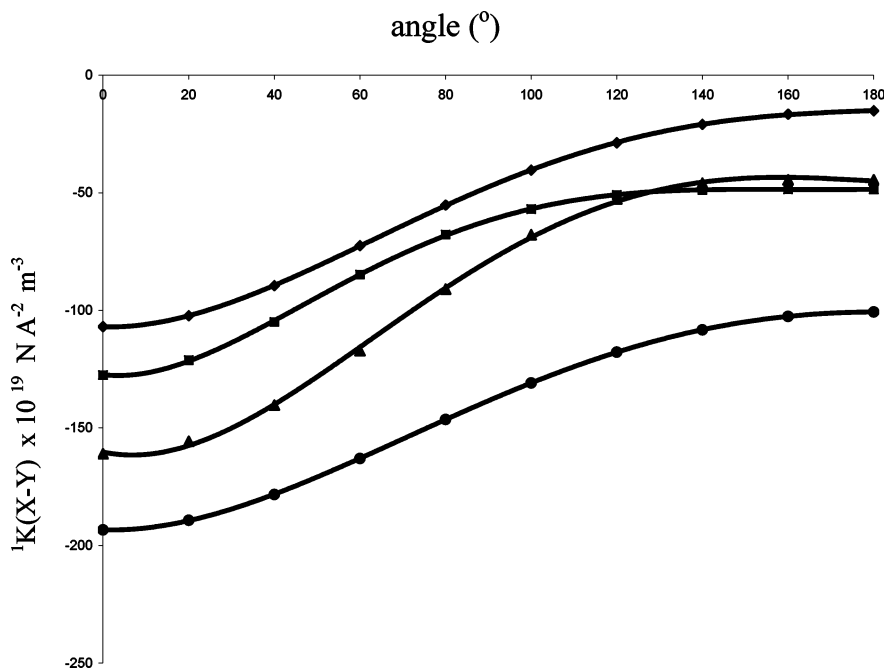


**Figure 10.** Variation of  ${}^1K(X-Y)$  for  $\text{H}_2\text{N-OH}$  (◆),  $\text{H}_2\text{N-SH}$  (▲),  $\text{H}_2\text{P-OH}$  (●), and  $\text{H}_2\text{P-SH}$  (■) with torsion angle.

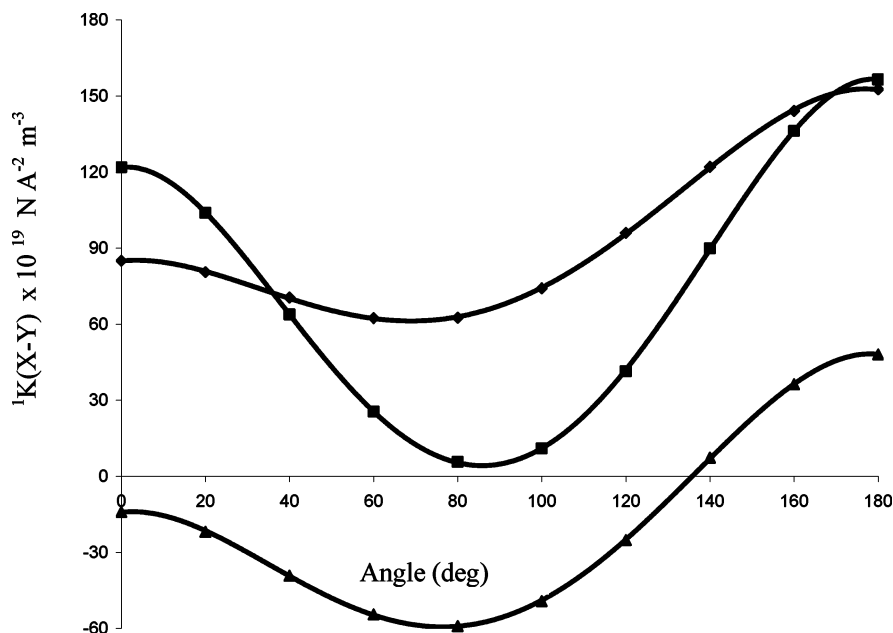
largest absolute value, followed by  $\text{H}_2\text{N-NH}_2$  and then  $\text{H}_2\text{P-PH}_2$ . At  $180^\circ$  when the lone pairs are “trans”, the differences among  ${}^1K(X-Y)$  values are much smaller.  $\text{H}_2\text{N-PH}_2$  still has the largest (negative) reduced coupling constant, while  $\text{H}_2\text{N-NH}_2$  and  $\text{H}_2\text{P-PH}_2$  have small, positive reduced N–N and P–P coupling constants. However, the reduced one-bond coupling constants  ${}^1K(X-Y)$  for these three molecules are negative and in violation of the Dirac Vector Model over most values of the dihedral angle.

Figure 10 presents the reduced coupling constants  ${}^1K(X-Y)$  for  $\text{H}_2\text{N-OH}$ ,  $\text{H}_2\text{N-SH}$ ,  $\text{H}_2\text{P-OH}$ , and  $\text{H}_2\text{P-SH}$  as a function of the dihedral angle.  ${}^1K(X-Y)$  is negative for all values of the dihedral angle and has its greatest absolute value when  $\theta = 0^\circ$ .  ${}^1K(X-Y)$  shows only a small dependence on the dihedral angle over the range between  $140$  and  $180^\circ$  and exhibits its smallest absolute value when  $\theta$  is equal to  $180^\circ$ . At this angle,

the lone pairs on X and Y are on opposite sides of the X–Y bond. At  $\theta = 0^\circ$ , the absolute value of  ${}^1K(X-Y)$  decreases with respect to X–Y in the order  $\text{P-O} > \text{N-S} > \text{P-S} > \text{N-O}$ ; that is, the reduced coupling constants are greater when X and Y are from different periods. Despite these differences, the similarities in the  ${}^1K(X-Y)$  curves for molecules  $\text{H}_2\text{X-YH}$  as a function of dihedral angle are apparent from Figure 10.

The variation of  ${}^1K(X-Y)$  with dihedral angle for molecules  $\text{HX-YH}$  is illustrated in Figure 11 and is dramatically different from the curves for  $\text{H}_2\text{X-YH}_2$  and  $\text{H}_2\text{X-YH}$ . Molecules  $\text{H}_2\text{X-YH}_2$  and  $\text{H}_2\text{X-YH}$  have their largest negative values at  $\theta = 0^\circ$  and tend to decrease smoothly as  $\theta$  increases to  $180^\circ$ . In contrast,  ${}^1K(X-Y)$  for  $\text{HO-OH}$  and  $\text{HS-SH}$  are positive for all values of the dihedral angle and have their largest values at  $\theta = 180^\circ$ , when the lone pairs on X and Y are trans with respect to the X–Y bond. Although  ${}^1K(\text{S-O})$  is negative initially, it





**Figure 11.** Variation of  ${}^1K(X-Y)$  for HO–OH ( $\blacklozenge$ ), HO–SH ( $\blacktriangle$ ), and HS–SH ( $\blacksquare$ ) with torsion angle.

changes sign at an angle of about  $130^\circ$ .  ${}^1K(X-Y)$  for all molecules in this set have minimum values as  $\theta$  approaches  $90^\circ$  at which point the X–H and Y–H bonds lie in perpendicular planes in a gauche conformation. Although the minimum for HO–OH at this angle is very shallow, the overall shapes of the three curves are similar. The differences in the  ${}^1K(X-Y)$  curves for molecules HX–YH compared with the corresponding curves for  $H_2X-YH_2$  and  $H_2X-YH$  are a direct consequence of the increased importance of the PSO and SD terms for molecules HX–YH.

### Conclusions

Ab initio EOM-CCSD calculations have been carried out to determine the variation of one-bond X–Y coupling constants  ${}^1J(X-Y)$  and its components as a function of dihedral angle for molecules  $H_2X-YH_2$ ,  $H_2X-YH$ , and HX–YH for X, Y =  ${}^{15}N$ ,  ${}^{17}O$ ,  ${}^{31}P$ , and  ${}^{33}S$ , molecules which have at least one lone pair of electrons on both X and Y. The results of these calculations support the following statements:

(1) The reduced FC terms for all molecules are negative and decrease in absolute value as the dihedral angle  $\theta$  increases from  $0^\circ$  to  $180^\circ$ . This rotation changes the orientation of the lone pairs relative to the X–Y bond from “cis” to “trans”. The reduced PSO and SD terms are of opposite sign from the FC term and have their maximum or minimum values at the gauche conformation.

(2) For molecules  $H_2X-YH_2$  which have one lone pair of electrons on X and another on Y, the shape of the  ${}^1J(X-Y)$  curve as a function of dihedral angle is essentially the shape of the FC curve. The PSO and SD terms are relatively small for  $H_2N-NH_2$  and  $H_2N-PH_2$  but assume increased importance as  $\theta$  approaches  $180^\circ$  and the FC term decreases. In contrast, the PSO and SD terms make relatively large contributions to the total coupling constant for  $H_2P-PH_2$ . These terms have their minimum absolute value at the gauche conformation for all molecules in this set.

(3) For molecules  $H_2X-YH$  which have one lone pair of electrons on X and two lone pairs on Y, the sign of  ${}^1J(X-Y)$  is the same as the sign of the FC term, which is the dominant term for all values of the dihedral angle. The signs of the PSO and SD terms are opposite that of the FC term. However, in

contrast to molecules  $H_2X-YH_2$ , the PSO and SD terms have their maximum absolute values at the gauche conformation.

(4) The variation in  ${}^1J(X-Y)$  with dihedral angle for molecules HX–YH, which have two lone pairs on each atom, is quite different from that observed for  $H_2X-YH_2$  and  $H_2X-YH$ . While the signs of the PSO and SD terms are opposite that of the FC term for HO–OH, the PSO and SD terms dominate, with the result that the sign of  ${}^1J(O-O)$  is determined by the signs of these terms and is positive. For all molecules in this set, the FC terms decrease in absolute value with increasing  $\theta$ , while PSO and SD terms assume increased importance over the entire range of dihedral angles. These terms are of opposite sign from the FC term and have their minimum absolute values at the gauche conformation where  ${}^1J(X-Y)$  also has its minimum absolute value. However, for HO–SH and HS–SH, the PSO and SD terms tend to cancel the FC term, with the result that  ${}^1J(O-S)$  and  ${}^1J(S-S)$  are relatively small over the entire range of dihedral angles.

(5) The reduced coupling constants  ${}^1K(X-Y)$  are readily grouped into families by formula, that is, by the number of electron pairs on X and Y.

(a) Curves showing the variation of  ${}^1K(X-Y)$  for molecules  $H_2X-YH_2$  have similar shapes, are large and negative at  $\theta = 0^\circ$ , and approach zero as  $\theta$  approaches  $180^\circ$ .  ${}^1K(P-P)$  is distinctive insofar as its maximum absolute value is not at  $0^\circ$  due to the increased importance of the PSO and SD terms for  $H_2P-PH_2$  compared with the other two molecules in this set. The reduced one-bond coupling constants are negative for most values of  $\theta$ .

(b) The reduced coupling constants for molecules  $H_2X-YH$  are negative over the entire range of dihedral angles. The  ${}^1K(X-Y)$  curves have similar shapes, exhibiting their largest negative values at  $\theta = 0^\circ$  and approaching zero as  $\theta$  approaches  $180^\circ$ .

(c) In contrast to the reduced coupling constants for the previous two sets of molecules, the reduced coupling constants  ${}^1K(O-O)$  and  ${}^1K(S-S)$  are positive for all values of  $\theta$ . Although  ${}^1K(O-S)$  is negative for most values of this angle, the shapes of the  ${}^1K(X-Y)$  curves for molecules HX–YH are similar, exhibit minimum absolute values at the gauche conformation, and maximum positive values at  $\theta = 180^\circ$ .

(d) For all  ${}^1\text{K}(\text{X}-\text{Y})$ , the order of curves within a given family is such that the curve for molecules in which X and Y are from different rows of the periodic table are more negative (less positive) than the reduced coupling constants for molecules in which X and Y are from the same period.

**Acknowledgment.** The continuing support of the Ohio Supercomputer Center is gratefully acknowledged. This work was carried out with financial support from the Ministerio de Ciencia y Tecnología (Project No. BQU2003-01251).

**Supporting Information Available:** Table S1 contains the total coupling constants  ${}^1\text{J}(\text{X}-\text{Y})$  as well as the PSO, FC, and SD terms as a function of dihedral angle for all of the molecules  $\text{H}_m\text{X}-\text{YH}_n$ . Full citations for refs 14 and 21 are also given. This information is available free of charge via the Internet at <http://pubs.acs.org>.

## References and Notes

- (1) Dalton, L. *Chem. Eng. News* **2003**, *81*, 37. The 125 Most Cited JACS publications. No. 17: Karplus, M. *J. Am. Chem. Soc.* **1963**, *85*, 2870.
- (2) Contreras, R. H.; Barone, V.; Facelli, J. C.; Peralta, J. E. Advances in Theoretical and Physical Aspects of Spin-Spin Coupling Constants. *Annu. Rep. NMR Spectrosc.* **2003**, *51*, 167.
- (3) Del Bene, J. E.; Elguero, J. *J. Phys. Chem. A* **2006**, *110*, 12543.
- (4) Pople, J. A.; Binkley J. S.; Seeger, R. *Int. J. Quantum Chem., Quantum Chem. Symp.* **1976**, *10*, 1.
- (5) Krishnan, R.; Pople, J. A. *Int. J. Quantum Chem.* **1978**, *14*, 91.
- (6) Bartlett, R. J.; Silver, D. M. *J. Chem. Phys.* **1975**, *62*, 3258.
- (7) Bartlett, R. J.; Purvis, G. D. *Int. J. Quantum Chem.* **1978**, *14*, 561.
- (8) Hehre, W. J.; Ditchfield, R.; Pople, J. A. *J. Chem. Phys.* **1982**, *56*, 2257.
- (9) Hariharan, P. C.; Pople, J. A. *Theor. Chim. Acta* **1973**, *238*, 213.
- (10) Spitznagel, G. W.; Clark, T.; Chandrasekhar, J.; Schleyer, P. v. R. *J. Comput. Chem.* **1982**, *3*, 3633.
- (11) Clark, T.; Chandrasekhar, J.; Spitznagel, G. W.; Schleyer, P. v. R. *J. Comput. Chem.* **1983**, *4*, 294.
- (12) Dunning, T. H., Jr. *J. Chem. Phys.* **1989**, *90*, 1007.
- (13) Woon, D. E.; Dunning, T. H., Jr. *J. Chem. Phys.* **1995**, *103*, 4572.
- (14) Frisch, M. J.; et al. *Gaussian03*; Gaussian, Inc.: Wallingford, CT, 2004.
- (15) Perera, S. A.; Sekino, H.; Bartlett, R. J. *J. Chem. Phys.* **1994**, *101*, 2186.
- (16) Perera, S. A.; Nooijen, M.; Bartlett, R. J. *J. Chem. Phys.* **1996**, *104*, 3290.
- (17) Perera, S. A.; Bartlett, R. J. *J. Am. Chem. Soc.* **1995**, *117*, 8476.
- (18) Perera, S. A.; Bartlett, R. J. *J. Am. Chem. Soc.* **1996**, *118*, 7849.
- (19) Schäfer, A.; Horn, H.; Ahlrichs, R. *J. Chem. Phys.* **1992**, *97*, 2571.
- (20) Kirpekar, S.; Jensen, H. J. Aa.; Oddershede, J. *J. Chem. Phys.* **1994**, *188*, 171.
- (21) Stanton, J. F.; et al. *ACES II, a program product of the Quantum Theory Project*; University of Florida: Gainesville, FL.
- (22) Stothers, J. B. *Carbon-13 NMR Spectroscopy*; Academic Press: New York, 1972; p 371.
- (23) Wolfe, S. *Acc. Chem. Res.* **1972**, *5*, 102.
- (24) (a) Yamaguchi, A.; Ichishima, I.; Shimanouchi, T.; Mizushima, S. *J. Chem. Phys.* **1959**, *31*, 843. (b) Morina, Y.; Ijima, T.; Murata, Y. *Bull. Chem. Soc. Jpn.* **1960**, *33*, 46. (c) Kasuya, T.; Kojima, T. *J. Phys. Soc. Jpn.* **1963**, *18*, 364.
- (25) Deslonchamps, P. *Stereoelectronic Effects in Organic Chemistry*; Pergamon Press: Oxford, U.K., 1983.
- (26) Lynden-Bell, R. M.; Harris, R. K. *Nuclear Magnetic Resonance Spectroscopy*; Appleton Century Crofts: New York, 1969.
- (27) Del Bene, J. E.; Elguero, J. *J. Chem. Phys. Lett.* **2003**, *382*, 100.
- (28) Gräfenstein, J.; Cremer, D. *J. Chem. Phys. Lett.* **2004**, *383*, 332.
- (29) Pecul, M.; Helgaker, T. *Int. J. Mol. Sci.* **2003**, *4*, 143.
- (30) Berger, S.; Braun, S.; Kalinowski, H.-O. *NMR Spectroscopy of the Nonmetallic Elements*; John Wiley & Sons: Chichester, U.K., 1997; p 274.
- (31) Reference 28, p 281.
- (32) Reference 28, p 948.